

Rate for $\mu^- \rightarrow e^- + e^- + e^+$ in two $SU(2) \times U(1)$ models*

S. M. Barr and S. Wandzura

Department of Physics, Joseph Henry Laboratories, Princeton University, Princeton, New Jersey 08540

(Received 22 February 1977; revised manuscript received 14 March 1977)

The rate for the decay $\mu^- \rightarrow e^- + e^- + e^+$ is calculated in the Wilczek-Zee and Cheng-Li models to first order in $\Delta m^2/M_W^2$, where Δm^2 is the difference of the squares of the heavy-lepton masses. The muon-number-violating μ -capture process $\mu + \text{nucleus} \rightarrow e + \text{nucleus}$ is discussed.

I. INTRODUCTION

Renewed interest in the possibility of muon-number nonconservation has led to the development of several models^{1,2,3} in which such processes as $\mu \rightarrow e + \gamma$ and $\mu \rightarrow e + e + \bar{e}$ occur, but at a rate greatly suppressed compared to ordinary μ decay. It has been previously noted that the ratio $\Gamma(\mu \rightarrow e + e + \bar{e})/\Gamma(\mu \rightarrow e + \gamma)$ is sensitive to the details of the model. In particular it has been observed that it tends to have a larger value in the Wilczek-Zee model with doubly charged heavy leptons than in the model of Cheng and Li with neutral heavy leptons. Wilczek and Zee² have already estimated this ratio for their model from the contribution of the dominant graph. In Sec. II we extend this calculation, keeping all terms of order $(m_k^2 - m_h^2)/M_W^2$ where m_k and m_h are the heavy-lepton masses. In Sec. III we calculate this ratio for the Cheng-Li model as well. And in Sec. IV we discuss the muon-number-violating μ -capture process $\mu + \text{nucleus} \rightarrow e + \text{nucleus}$ which may provide another sensitive test of the theory.

II. CALCULATION OF $\Gamma(\mu \rightarrow 3e)/\Gamma(\mu \rightarrow e + \gamma)$

The $\mu e \gamma$ vertex can be written in the form

$$\Gamma_\lambda(\mu e \gamma) = -ie\bar{u}_L(e) \left[F_1^{(\gamma)}(q^2)\gamma_\lambda + F_2^{(\gamma)}(q^2)\frac{i\sigma_{\lambda\nu}q^\nu}{m_\mu} + F_3^{(\gamma)}(q^2)q_\lambda \right] u(\mu), \quad (1)$$

where, by gauge invariance, $F_1^{(\gamma)}(0) = 0$ and $F_3^{(\gamma)}$ does not contribute to the decay; so that we can write $F_1^{(\gamma)}(q^2) = q^2 F_1^{(\gamma)'}$. The $\mu e Z$ vertex may be written similarly as

$$\Gamma_\lambda(\mu e Z) = -i(g^2 + g'^2)^{1/2} \bar{u}_L(e) \times \left[F_1^{(Z)}(q^2)\gamma_\lambda + F_2^{(Z)}(q^2)\frac{i\sigma_{\lambda\nu}q^\nu}{m_\mu q^2} + F_3^{(Z)}(q^2)q_\lambda \right] u(\mu), \quad (2)$$

where g and g' are defined in the usual way. To our order of approximation only $F_1^{(Z)}(0)$ is significant because of the Z boson's assumed high mass.

Neutral-unphysical-Higgs-boson exchange is not important as the $s^0 e^+ e^-$ coupling is proportional to the electron mass. The physical Higgs bosons are assumed to have sufficiently large mass so that they may be neglected (except, as will be seen, they must be taken into account to regulate one of the diagrams involving unphysical Higgs bosons).

The diagrams that contribute to $\Gamma_\lambda(\mu e \gamma)$ are shown in Figs. 1(a)–1(f). The evaluation of these diagrams is straightforward and has been performed. (We are calculating in the 't Hooft-Feynman gauge.) The results are

$$F_1^{(\gamma)' } = \frac{\sqrt{2} G_\mu \sin\phi \cos\phi}{8\pi^2} \left[2(k-h) - \frac{4}{3} \ln(k/h) \right], \quad (3)$$

$$F_2^{(\gamma)' } = m_\mu^2 \frac{\sqrt{2} G_\mu \sin\phi \cos\phi}{8\pi^2} \left(-\frac{5}{4} \right) (k-h),$$

where G_μ is the Fermi coupling constant, which in

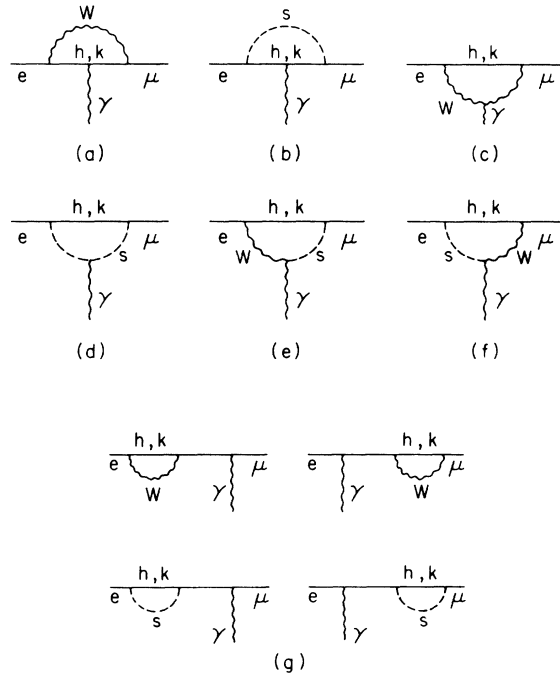


FIG. 1. Diagrams contributing to $\Gamma_\lambda(\mu e \gamma)$.

this theory is $2\sqrt{2}g^2/M_w^2$, ϕ is the heavy-lepton mixing angle analogous to the Cabibbo angle, and $h \equiv (m_h/M_w)^2$, $k \equiv (m_k/M_w)^2$. The diagrams for the Z vertex, $\Gamma_\lambda(\mu e Z)$ are, of course, of the same type as shown in Fig. 1. A simple device⁴ facilitates the calculation of $F_1^{(Z)}(0)$. Since by gauge invariance the sum of the contributions to $F_1^{(\gamma)}(0)$ from the graphs 1(a)–1(g) is identically zero we may clearly subtract from each Z vertex graph a constant times the corresponding γ vertex graph without affecting the value of $F_1^{(Z)}(0)$ for the sum of all the graphs. That is, if F_{1i} stands for the contribution to F_1 from graph i , we have

$$\sum_i F_{1i}^{(Z)}(0) = \sum_i \left[F_{1i}^{(Z)}(0) - \frac{g'}{g} F_{1i}^{(\gamma)}(0) \right]. \quad (4)$$

Thus we need to calculate this “remainder” for each diagram. This is equivalent to using the “effective” $Z\mu e$ couplings given in Table I and Fig. 2. When this is done, it is found that the diagrams of type 1(g) are exactly canceled, and the divergent part of the diagram of type 1(b) is also canceled. However, the diagram of type 1(d) remains divergent. In order to cancel this divergence, it is actually necessary to take into account the similar diagrams involving the charged physical Higgs particle. This interesting feature of such calculations in vector models was first pointed out by Yevick.⁵ The final result for the Z vertex diagrams is

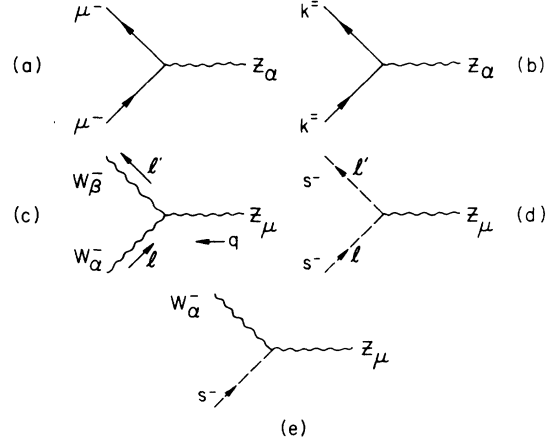


FIG. 2. Z vertices. The appropriate Feynman rules are given in Table I.

$$F_1^{(Z)}(0) = \frac{\sqrt{2} G_\mu \sin\phi \cos\phi}{8\pi^2} M_w^2 (k-h) \times \left[-4 - \frac{2}{\xi} - 2f(k, h) - \left(1 - \frac{1}{2\xi}\right) \delta(M_H/M_w) \right], \quad (5)$$

where

$$\delta(x) \equiv \frac{x^2+1}{x^2-1} \ln x - 1,$$

$$f(k, h) \equiv \frac{k \ln k - h \ln h}{k-h} - 1 \approx \ln k,$$

and where M_H is the mass of this singly charged physical Higgs particle, and ξ hereafter means

TABLE I. The effective Feynman rules used to evaluate the Z -boson vertices in the Wilczek-Zee model.

Vertex	Lagrangian Feynman rule	“Effective” Feynman rule
(a) $Z\mu\mu$	$-i \frac{g'^2}{(g^2+g'^2)^{1/2}} \bar{\mu} \gamma_\alpha \mu$	0
(b) Zkk	$i \frac{g^2-g'^2}{(g^2+g'^2)^{1/2}} \bar{k}_L \gamma_\alpha k_L - i \frac{2g'^2}{(g^2+g'^2)^{1/2}} k_R \gamma_\alpha k_R$	$i (g^2+g'^2)^{1/2} \bar{k}_L \gamma_\alpha k_L$
(c) ZWW	$-i \frac{g^2}{(g^2+g'^2)^{1/2}} [g_{\alpha\beta}(l+l')_\mu - l_\beta g_{\mu\alpha} - l'_\alpha g_{\mu\beta} + g_{\alpha\mu} q_\beta q_\alpha]$	$-i (g^2+g'^2)^{1/2} [g_{\alpha\beta}(l+l')_\mu - l_\beta g_{\mu\alpha} - l'_\alpha g_{\mu\beta} + g_{\alpha\mu} q_\beta - g_{\beta\mu} q_\alpha]$
(d) Zss	$+i \frac{1}{(g^2+g'^2)^{1/2}} \left(g^2 - \frac{g^2+g'^2}{2\xi} \right) (l+l')_\mu$	$+i \frac{1}{(g^2+g'^2)^{1/2}} \left(g^2 + g'^2 - \frac{g^2+g'^2}{2\xi} \right) (l+l')_\mu$
(e) ZsW	$+i \frac{g^2}{(g^2+g'^2)^{1/2}} M_w \left(1 - \frac{M_Z^2}{M_w^2} \right) g_{\alpha\mu}$	$\frac{+i}{(g^2+g'^2)^{1/2}} \left(g^2 + g'^2 - \frac{M_Z^2}{M_w^2} \right) M_w g_{\alpha\mu}$

$M_W^2/M_Z^2 \cos^2\theta_w$, which is 1 in the Weinberg-Salam model but a free parameter here, subject to the constraint $\xi \geq \frac{1}{2}$.

In addition to the vertex diagrams there are six box diagrams which contribute to the rate. They

$$M_b = ie^2 \bar{u}_L(e_1) F_b \gamma^\lambda u(\mu) \bar{u}_L(e_2) \gamma_\lambda v_L(e^+) - (1 \rightarrow 2), \quad (7)$$

$$F_b = \frac{\sqrt{2} G_\mu \sin\phi \cos\phi}{8\pi^2} \frac{1}{\sin^2\theta_w} \left\{ \frac{5}{2}(k-h) + 3[k \ln(k) - h \ln(h)] + \cos 2\phi \left[\frac{1}{2}(h+k) - kh \ln(k/h)/(k-h) \right] \right\},$$

which vanishes, as it must, for $k=h$. The total matrix element thus may be written

$$M = ie^2 \bar{u}_L(e_1) \left(A \gamma_\lambda + F_2^{(\gamma)} \frac{i\sigma_{\lambda\nu} q_1^\nu}{m_\mu q_1^2} \right) u(\mu) \bar{u}(e_2) \gamma_\lambda v(e^+) + ie \bar{u}_L(e_1) F_b \gamma^\lambda u(\mu) \bar{u}_L(e_2) \gamma_\lambda v_L(e^+) - (1 \rightarrow 2), \quad (8)$$

where

$$A = F_1^{(\gamma)}, - \frac{1}{M_Z^2 \cos^2\theta_w} F_1^{(Z)}(0).$$

The rate⁶ in terms of the previously defined form factors is ($G_b \equiv 0$ here and will only be important when we discuss the Cheng-Li model)

$$\Gamma(\mu \rightarrow 3e) = \frac{m_\mu^5 \alpha^2}{32\pi} \left[|A|^2 - 4 \operatorname{Re} A^* F_2^{(\gamma)}/m_\mu^2 + \frac{16}{3} \ln(m_\mu/2m_e) |F_2^{(\gamma)}|^2/m_\mu^4 + \frac{2}{3} |F_b|^2 + \frac{4}{3} \operatorname{Re} A^* F_b - \frac{8}{3} \operatorname{Re} F_b^* F_2^{(\gamma)}/m_\mu^2 + \frac{1}{3} |G_b|^2 + \frac{2}{3} \operatorname{Re} A^* G_b - \frac{4}{3} \operatorname{Re} G_b^* F_2^{(\gamma)}/m_\mu^2 \right], \quad (9)$$

the rate for $\mu \rightarrow e + \gamma$ is

$$\Gamma(\mu \rightarrow e + \gamma) = \frac{75}{32} \frac{\alpha}{\pi} \sin^2\phi \cos^2\phi (k-h)^2 \Gamma_\mu, \quad (10)$$

where $\Gamma_\mu = m_\mu^5 G_\mu^2 / 192\pi^3$ is the rate for ordinary μ decay. Thus the ratio of rates assumes the form

$$\frac{\Gamma(\mu \rightarrow 3e)}{\Gamma(\mu \rightarrow e + \gamma)} = \frac{2}{25} \frac{\alpha}{\pi} \left(a^2 + 5a + \frac{25}{3} \ln \frac{m_\mu}{2m_e} + \frac{2}{3} b^2 + \frac{4}{3} ab + \frac{10}{3} b \right)$$

$$a = -\frac{4}{3} \frac{\ln(k-h)}{k-h} + 4 + \xi \left[4 + 2f(k, h) - \delta \left(\frac{M_H}{M_W} \right) \left(1 - \frac{1}{2\xi} \right) \right],$$

$$b = \frac{1}{\sin^2\theta_w} \left\{ \frac{5}{2} + 3(k-h \ln h)/(k-h) + \cos 2\phi \left[\frac{k+h}{2(k-h)} - \frac{kh}{(k-h)^2} \ln(k/h) \right] \right\}. \quad (11)$$

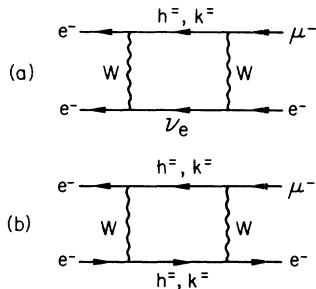


FIG. 3. The box diagrams. Notice that (b) represents four distinct diagrams.

are shown in Fig. 3. The box diagrams with one or both W 's replaced by unphysical Higgs particles, s^\pm , are down by powers of (m_μ/m_h) . The matrix-element contribution from these graphs is easily calculated at small external momenta and is

If we include only the dominant contribution then for $k \approx h$ the ratio is simply²

$$\frac{\Gamma(\mu \rightarrow 3e)}{\Gamma(\mu \rightarrow e + \gamma)} \approx \frac{32}{225} \frac{\alpha}{\pi} \left(\frac{M_W}{m_h} \right)^4. \quad (12)$$

Bounds may be placed on $\sin^2\theta_w$ by neutrino-electron scattering data⁷:

$$0.06 \leq \xi \sin^2\theta_w \leq 0.35. \quad (13)$$

Some results of a numerical calculation of the ratio of rates are shown in Fig. 4, where we plot

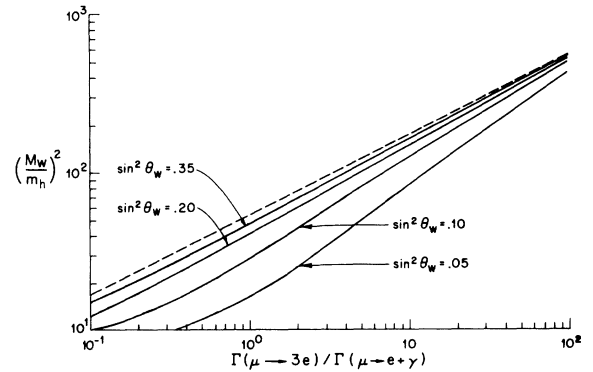


FIG. 4. The ratio of rates $\Gamma(\mu \rightarrow 3e)/\Gamma(\mu \rightarrow e + \gamma)$ for the Wilczek-Zee model is plotted versus the square of the W mass over the heavy-lepton mass, for the case where $m_h \approx m_k$. Each line represents constant Weinberg angle. The dotted line is the approximation given in Eq. (12).

$\Gamma(\mu - 3e)/\Gamma(\mu - e + \gamma)$ versus $(M_w/m_h)^2$ for various Weinberg angles. In the plot we have set $(k-h)/(k+h) \ll 1$ and ϕ small. The ratio is actually fairly insensitive to these parameters. We have also set $\xi = \frac{1}{2}$ in the plot. It may be seen from considering Eq. (11) that this value of ξ gives a lower bound on the ratio of rates, at least if the approximations we have been making are assumed to be valid: Since Δ_m^2/M_w^2 is assumed small, it is safe to say that $4 + 2f(k, h) > 0$, and $\delta(M_H/M_w) \geq 0$. As can be seen from the graphs, the estimate given in Eq. (12) is quite accurate except for small values of $\sin^2\theta_w$ and large values of the heavy-lepton masses. Notice that the ratio is actually *larger* than given by Eq. (12).

III. THE CHENG-LI MODEL

The diagrams which contribute to the decay $\Gamma(\mu - 3e)$ in the Cheng-Li¹ model are quite similar to those we have discussed already. However, it is important to note that, because of the neutrality of the heavy leptons in this theory, the diagrams corresponding to Figs. 1(a) and 1(b) do not appear. Since the dominant contribution in the Wilczek-Zee model to $\mu - 3e$ came from Fig. 1(a) we may expect that we will get a lower rate in the Cheng-Li model. The calculation parallels closely that outlined in Sec. II, so we will only state the results. The matrix element is of the form

$$\begin{aligned} \mathfrak{M} = & ie^2 \bar{u}_R(e_1) \left(A \gamma^\lambda + F_2^{(\gamma)} \frac{i \sigma_{\lambda\nu} q_1^\nu}{m_\mu q_1} \right) u(\mu) \bar{u}(e_2) \gamma_\lambda v(e^*) \\ & + ie^2 \bar{u}_R(e_1) F_b \gamma^\lambda u(\mu) \bar{u}_R(e_2) \gamma_\lambda v_R(e^*) \\ & + ie^2 \bar{u}_R(e_1) G_b \gamma^\lambda u(\mu) \bar{u}_L(e_2) \gamma_\lambda v_L(e^*) - (1 \rightarrow 2) \end{aligned} \quad (14)$$

with

$$\begin{aligned} A = & F_1^{(\gamma)'} + \frac{1}{2M_Z^2} \left(\frac{1}{\sin^2\theta_w} - \frac{1}{\cos^2\theta_w} \right) F_1^{(Z)}(0), \\ F_1^{(\gamma)'} = & C(n_2 - n_1), \\ F_2^{(\gamma)} = & m_\mu^2 C - \frac{5}{4}(n_2 - n_1), \\ F_1^{(Z)}(0) = & C \frac{M_W^2}{2} [8 + 2f(n_2, n_1)](n_2 - n_1), \\ F_b = & C \frac{1}{\sin^2\theta_w} \left\{ -\frac{3}{4}(n_2 - n_1) - \frac{1}{2}(n_2 \ln n_2 - n_1 \ln n_1) \right. \\ & \left. + \frac{1}{2} \cos 2\phi \left[\frac{n_2 + n_1}{2} - \frac{n_2 n_1}{n_2 - n_1} \ln(n_2/n_1) \right] \right\}, \\ G_b = & C \frac{1}{\sin^2\theta_w} [-2(n_2 - n_1) - 2(n_2 \ln n_2 - n_1 \ln n_1)], \\ C = & \frac{\sqrt{2} G_\mu \sin\phi \cos\phi}{8\pi^2}. \end{aligned} \quad (15)$$

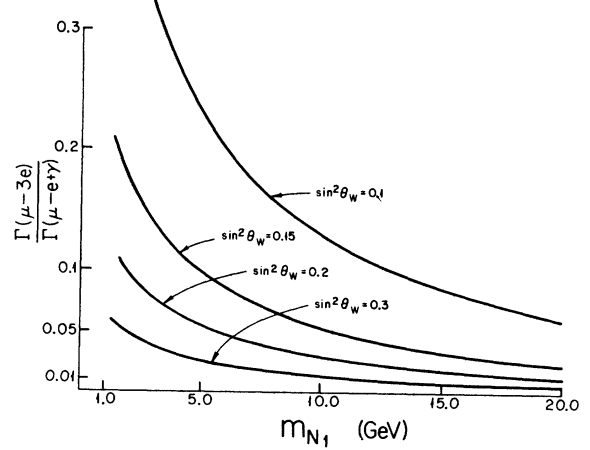


FIG. 5. The ratio $\Gamma(\mu - 3e)/\Gamma(\mu - e + \gamma)$ versus the mass of one of the neutral heavy leptons in the Cheng-Li model. Different lines represent different Weinberg angle. It is assumed that $m_{N_1} \approx m_{N_2}$ and that $M_w = M_Z \cos\theta_w$.

N_1, N_2 are the neutral heavy leptons of this theory and $n_1 \equiv (m_{N_1}/M_w)^2$, $n_2 \equiv (m_{N_2}/M_w)^2$. The rate is given by Eq. (9). The rate for $\mu - e + \gamma$ is the same as in the Wilczek-Zee model [see Eq. (10)]. The ratio of rates for the Cheng-Li model is plotted in Fig. 5 versus m_N . In this model, with one Higgs doublet, $\xi = 1$.

IV. MUON CAPTURE

Strict constraints may be placed on the Wilczek-Zee model by the μ -capture process on nucleus: $\mu^- + Z \rightarrow \mu^- + Z'$. Weinberg and Feinberg⁸ have calculated the branching ratio for this process when mediated by photon exchange only. This is a valid approximation in the Wilczek-Zee model as the dominant term comes from the photon vertex diagram shown in Fig. 1(a). A more complex form would result were we to include subdominant terms, as we would need to know the coupling to the nucleus of the neutral weak current and of the product of charged weak currents. The result of Weinberg and Feinberg is

$$\begin{aligned} \frac{\Gamma(\mu + Z \rightarrow e + Z')}{\Gamma(\mu + Z \rightarrow \nu + (Z - 1))} \\ = 384\pi^3 \alpha \left(\frac{\xi_0}{\xi_\beta} \right)^2 \frac{\alpha}{8\pi} \frac{2}{3} Z |F_{ZZ'}(m_\mu^2)|^2 \frac{1}{2C}, \end{aligned} \quad (16)$$

where, in our notation,

$$\xi_0^2 \simeq \frac{1}{4} m_\mu^4 |F_1'|^2, \quad \xi_\beta^2 = 2G_\mu^2 m_\mu^4,$$

and where

$$\begin{aligned} ZeF_{ZZ'}(q^2)/2\pi^3 \equiv \langle Z' | J_0^0(0) | Z \rangle, \\ C = \left(\frac{\langle \nu_N \rangle}{m_\mu} \right)^2 \left(1 - \frac{A - Z}{2A} \delta \right). \end{aligned} \quad (17)$$

Here $\nu_N \approx 0.75m_\mu$ is the mean neutrino momentum in all final states for ordinary μ capture. δ represents the inhibition of μ capture due to the Pauli principle; δ is approximately 3. C varies from 0.14 in the lightest nuclei to 0.05 for ^{208}Pb .

To the order of approximation we are discussing we may express this in the very useful form

$$\frac{\Gamma(\mu + Z \rightarrow e + Z')}{\Gamma(\mu + Z \rightarrow \nu + (Z-1))} = \frac{2}{3} Z |F_{ZZ'}(m_\mu^2)|^2 \frac{\Gamma(\mu \rightarrow 3e)}{\Gamma(\mu \rightarrow e + \nu + \bar{\nu})} \frac{1}{2C}. \quad (18)$$

The factor of $\frac{2}{3}$ comes from the fact that there are two identical particles in the final state of $\mu \rightarrow 3e$. Weinberg and Feinberg⁸ have estimated that the factor $Z |F_{ZZ'}(m_\mu^2)|^2$ attains a maximum value of about 6 for Cu and decreases for heavier nuclei to about 2.5 for Pb. At present the experimental limit^{8,9} on the μ -capture process

$$\frac{\Gamma(\mu + Z \rightarrow e + Z')}{\Gamma(\mu + Z \rightarrow \nu + (Z-1))} \lesssim 1.9 \times 10^{-8};$$

the present limit¹⁰ on $\mu \rightarrow 3e$ is

$$\frac{\Gamma(\mu \rightarrow 3e)}{\Gamma(\mu \rightarrow e + \nu + \bar{\nu})} \lesssim 1.9 \times 10^{-9},$$

so that an improvement in the measurement of μ capture could provide an important test of the Wilczek-Zee model where this branching ratio is expected to be larger than in the other models.

It is also to be noted that by observing the rare muon capture, $\mu + \text{nucleus} \rightarrow e + \text{nucleus}$, on polarized targets one may search for T -violating effects in weak interactions.

Note added. After completion of this work it was drawn to our attention that results given here for the Cheng-Li model had also been obtained by other authors, among whom are V. Barger and D. V. Nanopoulos, and T. P. Cheng and L-F. Li.

ACKNOWLEDGMENTS

The authors would like to thank W. Marciano, F. Wilczek, D. Yevick, and A. Zee for helpful discussions.

*Work supported in part by the National Science Foundation under Grant No. MPS75-22514.

¹T. P. Cheng and L.F. Li, Phys. Rev. Lett. **38**, 381 (1977); S. B. Treiman, F. Wilczek, and A. Zee, Phys. Rev. D **16**, 152 (1977).

²F. Wilczek and A. Zee, Phys. Rev. Lett. **38**, 531 (1977).

³J. D. Bjorken and S. Weinberg, Phys. Rev. Lett. **38**, 622 (1977).

⁴E. B. Bogomol'nyi, V. A. Novikov, and M. A. Shifman, Yad. Fiz. **23**, 825 (1976) [Sov. J. Nucl. Phys. **23**, 435 (1976)]. Another approach is adopted by M. K. Gaillard and B. W. Lee, Phys. Rev. D **10**, 897 (1974).

⁵D. Yevick, doctoral thesis, Princeton University, 1977 (unpublished).

⁶M. Bander and G. Feinberg, Phys. Rev. **119**, 1427 (1960). This contains the terms of Eq. (9) which do not depend on F_b or G_b .

⁷J. J. Sakurai, International School of Subnuclear Physics, Erice, Sicily, 1976 (unpublished); UCLA Report No. UCLA/76/TEP/21 (unpublished).

⁸S. Weinberg and G. Feinberg, Phys. Rev. Lett. **3**, 111, 244 (1959). S. Frankel, in *Muon Physics*, edited by V. W. Hughes (Academic, New York, 1975), Vol. II, p. 83.

⁹D. A. Bryman, M. Blecher, K. Gotow, and R. J. Powers, Phys. Rev. Lett. **28**, 1469 (1972).

¹⁰S. M. Korenchenko, B. F. Kostin, G. V. Mitsel'makher, K. G. Nekrasov, and V. S. Smirnov, Zh. Eksp. Teor. Fiz. **70**, 3 (1976) [Sov. Phys.—JETP **43**, 1 (1976)].